Race Simulation and Energy Management System for a Solar Car

Ege Uzun[1], Can Akman [1], Mustafa Çağşak[2], Ali Eren Dağ [1] and Alper Tolga Çalık[3]

[1]Electrical Engineering Department Istanbul Technical University, Turkiye
uzune18@itu.edu.tr, akmanc21@itu.edu.tr, daga22@itu.edu.tr
[2]Computer Engineering Department Istanbul Technical University, Turkey
cagsak22@itu.edu.tr
[3]Mechanical Engineering Department Istanbul Technical University, Turkey
calik@itu.edu.tr

Abstract

This study develops a race-simulation and energy-management framework for ArıbaX in the 24-hour iLumen European Solar Challenge. The method combines a tractive-force model, a surface-mounted PMSM torque formulation, an efficiency-map based power path, and a pack-level balance for current and state of charge. It uses routine telemetry from the motor controller, the MPPT units, and the BMS. With measured speed as input, the model predicts 57.278 Wh per lap versus 58.154 Wh measured . Across 11 laps, the mean signed difference is 1.19%, the mean absolute percentage error is 2.81%, and the RMSE is 1.95 Wh. This accuracy supports practical choices such as pace targets, quantifying regeneration and auxiliary loads, and planning charge stops. The framework is simple to deploy, easy to interpret, and adaptable, which supports strategist workflows where real time data adjustments are essential during endurance racing.

1. Introduction

Electric vehicles are central to sustainable mobility for their efficiency and emissions benefits. Within this space, solar cars form a distinct class where onboard photovoltaic energy directly supports propulsion and extends operation without external charging [1, 2]. Research and racing have accelerated advances in modeling, energy management, and component optimization, enabling credible assessments of aerodynamics, rolling resistance, motor efficiency, and photovoltaic behavior under real conditions [3, 4, 5]. Solar car competitions provide a proving ground to test strategies and refine designs for endurance events [6].

Istanbul Technical University Solar Car Team (ITU SCT), founded in 2004, has produced ten vehicles, including a four-seat car; the latest is ArıbaX. Across projects the team advanced electrical architecture, strategy, and telemetry, contributing design criteria, on-road performance simulation, and optimization-guided control [7, 8, 9]. This lineage underpins the present integration of high-fidelity modeling with real-time data.

Solar car races such as the iLumen European Solar Challenge (iESC) emphasize endurance and robust strategy. Unlike point-topoint events (e.g., the Bridgestone World Solar Challenge), iESC is a 24-hour, non-stop circuit race at Circuit Zolder; the winner completes the most laps. Weather is simpler to forecast on a closed track, yet constant cornering and overtakes change panel incidence and cause brief shading, complicating real-time estimation of solar input and MPPT behavior. Night time removes solar input, and the rules allow only a limited number of charge stops, which heightens the need for accurate online SOC and energy management. Fig. 1. shows Circuit Zolder, a representative testbed with elevation changes and fast corners.

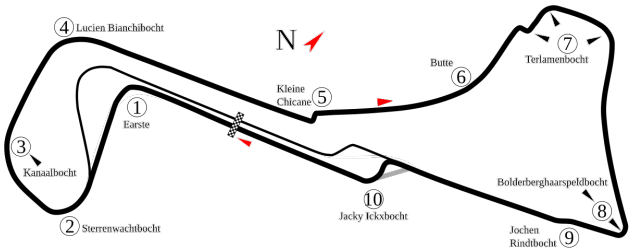

Fig. 1: Circuit Zolder (Belgium), race track of the iLumen European Solar Challenge

Traditional race planning often starts with offline simulations for speed and energy targets, but real conditions can erode a fixed plan: clouds reduce panel output, heat raises losses and can trigger derating, and traffic forces pace changes. To handle this, teams pair simulation with telemetry-based monitoring and decision tools—heuristic/metaheuristic optimizers, real-time tracking of power and SOC, and analyses that align model predictions with on-track data [10, 11]. Evidence shows that reliable data acquisition and parameter identification, used alongside simulation, enable timely adjustments and better outcomes [12, 13].

This study introduces a race–simulation and energy–management framework for ArıbaX in the 24-hour iESC, fusing physics-based tractive-force and battery models with real-time telemetry from the motor driver, BMS, and MPPTs to keep predicted power, energy, and SOC aligned with on-track behavior. The remainder of this paper is organized as follows: Section 2 details the vehicle and energy models (specifications, tractive forces, PMSM, pack balance, SOC); Section 3 presents results with per-lap and multi-lap validation; Section 4 concludes and outlines future work on race strategy optimization and charge planning.

2. Methodology and Simulation

In this section, a lap-based simulation is constructed using vehicle physics. Tractive demand is decomposed into aerodynamic drag, rolling resistance, grade, and inertia, then converted to shaft power and mapped through a surface-mounted PMSM efficiency map to obtain electrical power at the DC bus.

The workflow follows a digital-twin approach by aligning the simulation with real measurements.

2.1. ArıbaX Solar Car Specifications

The solar car used in this study is named ArıbaX. It is equipped with a 35-series LG MJ1 M35 battery pack, consisting of 420 cells and a total energy capacity of approximately 5.3 kWh. A three parallel MPPT (Maximum Power Point Tracking) system is used for efficient charging from the solar panels.

The motor test setup is configured to measure torque, speed, and phase currents under controlled load conditions. The motor and load are carefully aligned, sensors are calibrated, and the assembly is rigidly mounted to minimize vibration and measurement drift. The motor controller interface provides bus and RMS currents along with *d/q* voltages and currents, which are logged for subsequent analysis. The test bench used for these measurements is shown in Fig. 2.

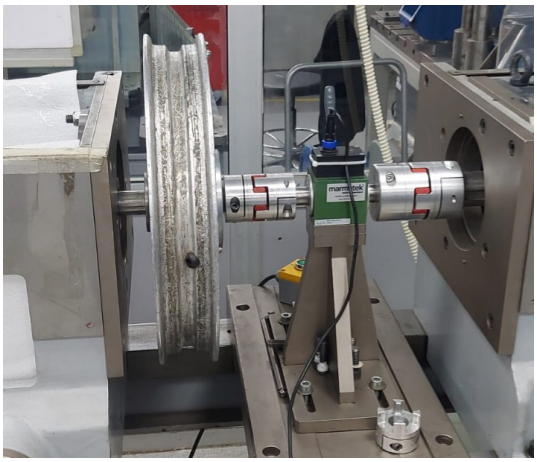

Fig. 2: Motor test bench used for torque, speed, and electrical variable measurements under controlled loading.

The logged data are post-processed to generate an efficiency map that relates operating points (speed–torque) to electrical-to mechanical conversion efficiency. This map is used to identify high-efficiency regions for race operation and to parameterize the simulation model with realistic loss characteristics. The resulting efficiency map derived from the bench measurements is shown in Fig. 3.

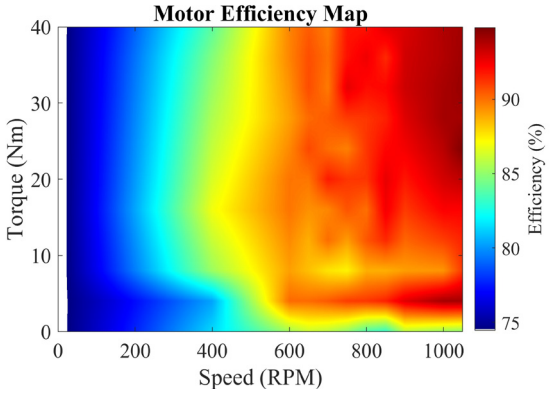

Fig. 3: Motor efficiency map obtained from bench measurements across speed–torque operating points.

2.2. Switch Selection and Loss Model

For the aerodynamic term, the air density, drag coefficient, frontal area, and vehicle speed are denoted by ρ, C_d, A, and v, respectively. The aerodynamic drag force is defined as in (1).

$$F_{drag} = \frac{1}{2} \rho C_d A v^2 \tag{1}$$

For the tire–road term, the rolling resistance coefficient, vehicle mass, and gravitational acceleration are denoted by C_r, M, and g, respectively. The rolling resistance force is given in (2).

$$F_{roll} = C_r M g \cos(\theta) \tag{2}$$

For grade effects, the track slope angle is denoted by θ. The gravitational component along the slope is computed as in (3).

$$F_{gravity} = M g \sin(\theta) \tag{3}$$

The vehicle mass and longitudinal acceleration are denoted by M and a, respectively. The inertial force associated with acceleration is defined as in (4).

$$F_{acceleration} = M a \tag{4}$$

The total tractive force required for the movement of the vehicle combining aerodynamic drag, rolling resistance, grade force, and the acceleration term is calculated as in (5).

$$F_{tractive} = F_{drag} + F_{roll} + F_{gravity} + F_{acceleration} \tag{5}$$

2.3. Power Transfer Between Battery, Motor, and Solar Array

The total tractive force and vehicle speed are denoted as $F_{tractive}$ and v. The propulsion power required at the wheels is computed as in (6), where $P_{required}$ is the mechanical shaft power (for a hub motor, $P_{required} = T\,\omega$ with $\omega = v/r$).

$$P_{required} = F_{tractive}\, v \tag{6}$$

The mechanical torque and angular speed are denoted by T and ω, the test-based machine efficiency map by $\eta_m(T,\omega)$, and the lumped converter (driver/inverter) efficiency by η_{drv}. P_{elec} denotes the DC electrical power at the inverter DC link. The electrical power at the DC side of the driver is obtained from the efficiency map as in (7), (8). Motor mode ($T \geq 0$), where the machine draws electrical power:

$$P_{elec} = \frac{T\,\omega}{\eta_m(T,\omega)\,\eta_{drv}} \tag{7}$$

Regeneration ($T < 0$), where electrical power is returned to the DC bus:

$$P_{elec} = \frac{\eta_m(T,\omega)}{\eta_{drv}}\, T \tag{8}$$

Where $T < 0$ makes $P_{elec} < 0$ (charging). When the efficiency map already includes driver losses, η_{drv} is set to 1 to avoid double counting.

The battery power, solar-array power from the MPPTs, electrical power demand for the motor, and auxiliary consumption are denoted as $P_{battery}$, P_{MPPT} , P_{elec}, and P_{aux}. Cable conduction losses are denoted by P_{cable} and represent I2R losses along the high current path. P_{MPPT} is the net electrical power from the solar arrays and P_{aux} includes fans, lights, and standby consumption of BMS, MPPT, driver, and display electronics. The pack-level balance used in simulation is written in (9).

$$P_{battery}=P_{MPPT}+P_{elec}+P_{aux}+P_{cable} \tag{9}$$

2.4. Battery Current and State of Charge

The battery pack power and the total number of cells are denoted by $P_{battery}(t)$ and N_{cells}, respectively. The per–cell power used in the simulation is obtained by ideal equal sharing as in (10).

$$P_{cell}(t)=\frac{P_{battery}(t)}{N_{cells}} \tag{10}$$

Identical cells and uniform current sharing are assumed. This approximation ignores cell-to-cell variation and thermal/electrical imbalance; it is appropriate here to establish a tractable link between pack measurements and cell-level dynamics.

The open-circuit voltage, internal resistance, and instantaneous per–cell power are denoted by $V_{oc}(t)$, $R_o(t)$, and $P_{cell}(t)$. The cell current used in the simulation is calculated as in (11), [14].

$$I_{cell}(t)=\frac{V_{oc}(t)-\sqrt{V_{oc}(t)^2-4\,R_o(t)\,P_{cell}(t)}}{2\,R_o(t)} \tag{11}$$

The sign convention is positive for discharge. The previous state of charge, time step, and rated cell capacity are denoted by SOC_{prev}, Δt, and C_{cell}. The discrete-time SOC update is written in (12), [14].

$$SOC(t)=SOC_{prev}-\frac{I_{cell}(t)\,\Delta t}{C_{cell}} \tag{12}$$

2.5. Vehicle, Battery, and Motor Parameters

Table 1. presents the key specifications of the vehicle, including its mass, frontal area, drag coefficient, rolling resistance coefficient, and battery parameters. These parameters are used in the simulation to calculate the forces, power, and energy consumption of ArıbaX.

Table 2. provides the characteristics of the battery cells, including the state of charge (SOC), open-circuit voltage (Voc), and internal resistance (Rint). These values are used to calculate the current and SOC dynamically in the simulation.

Table 1. Vehicle, battery, and motor parameters.

Parameter	Value	Unit	Description
M	250	kg	Vehicle and driver mass
A	0.9	m2	Frontal area
C_d	0.15	-	Aerodynamic drag coefficient
C_r	0.006	-	Rolling resistance coefficient
r	0.285	m	Wheel radius
Auxiliary Power	60	W	Electronics and fans
Cell Capacity	3.5	Ah	Single battery cell capacity
Number of Cells	420	-	Total number of cells
Pack Capacity	≈5.3	kWh	Total energy capacity
Solar Array Area	4	m2	Total solar panel area
Kt	0.9	Nm/A	Motor torque constant
p	20	-	Number of pole pairs
λ_m	≈ 0.03	Wb	Permanent-magnet flux linkage
Rated Motor Power	1.8	kW	Continuous rated power

Table 2. Battery Cell Characteristics [15].

SOC	Voc (V)	Rint (Ω)
1.000	4.21	0.070
0.954	4.12	0.070
0.909	4.09	0.076
0.818	4.04	0.102
0.727	3.93	0.086
0.636	3.85	0.084
0.545	3.75	0.092
0.454	3.66	0.102
0.364	3.60	0.097
0.273	3.50	0.082

2.6. PMSM Electromechanical Model and Pack Power Balance

In real time, electromechanical quantities are inferred from dq-frame signals reported by the motor driver together with pack and MPPT telemetry. The number of pole pairs, permanent-magnet flux linkage, and quadrature current are denoted by p, λ_m, and i_q, respectively. The torque generated by the surface-mounted PMSM is calculated as in (13).

$$T_e=\frac{3}{2}\,p\,\lambda_m\,i_q \tag{13}$$

The d- and q-axis voltages and currents measured by the driver are denoted by V_d, V_q, i_d, and i_q. The instantaneous electrical power at the machine terminals is written in (14).

$$P_{motor}=\frac{3}{2}\left(V_d\,i_d+V_q\,i_q\right) \tag{14}$$

The battery-side power, MPPT power, motor electrical power, auxiliary consumption, and aggregate losses are denoted by $P_{battery}$, P_{MPPT} , P_{motor}, P_{aux}, and P_{losses}. The real-time pack power balance is given in (15).

$$P_{battery}=P_{MPPT}+P_{motor}+P_{aux}+P_{losses} \tag{15}$$

The aggregate loss term includes cable conduction losses and motor driver conversion losses, denoted by P_{cable} and $P_{motordriver}$, respectively. This decomposition is stated in (16).

$$P_{losses}=P_{cable}+P_{motordriver} \quad (16)$$

3. Results and Discussion

The solar car's CAN network links the battery management system (BMS), SOC calculation unit, motor controller, and three MPPTs, streaming measurements to the driver display and logging them for analysis. The Telemetry Control Unit (TCU) shown in Fig. 4. aggregates all CAN frames, time-stamps them with a unified clock, and performs light edge computations. It also filters outliers, aligns asynchronous streams (BMS, MPPT, motor driver), and buffers data locally to prevent loss during cellular dropouts.

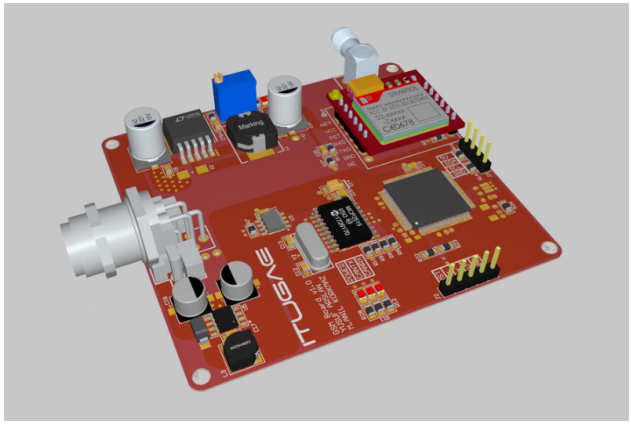

Fig. 4: Telemetry Control Unit (TCU)

Fig. 5. shows the interface used during testing, where battery voltage and SOC, motor power, and array output are visualized to monitor trends and flag deviations from the simulation in real time.

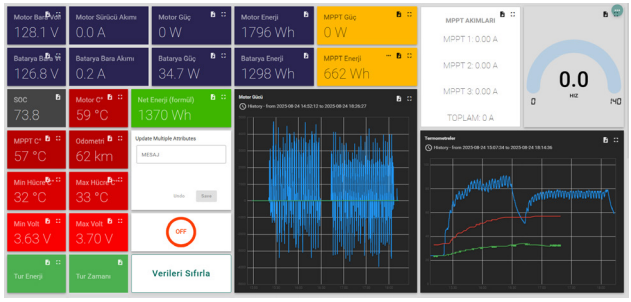

Fig. 5: User interface visualizing battery, motor, and MPPT

To resolve these telemetry streams, the simulation outputs for ArıbaX were compared with on-track measurements to check consistency. Fig. 6. expresses speed and motor power and Fig. 7. presents the corresponding SOC and pack current traces for the same lap.

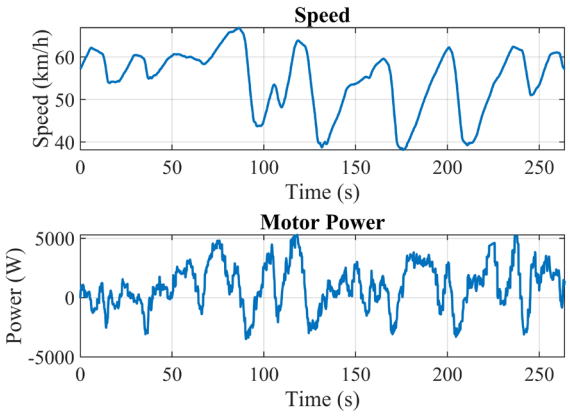

Fig. 6: Speed and motor power over time obtained from the simulation.

Fig. 7. shows the corresponding SOC and pack current. Read together, these figures verify that the model captures acceleration, cruise, coasting, and regeneration behavior and help locate any prediction measurement gaps.

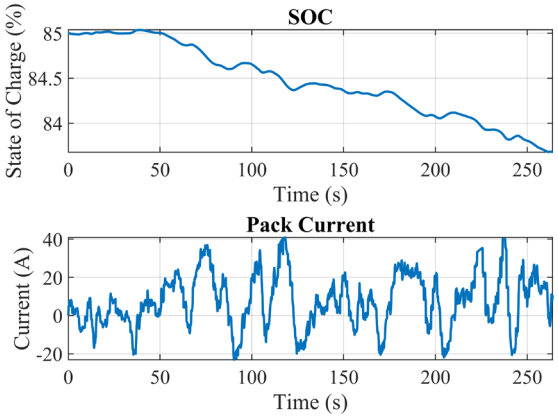

Fig. 7: Battery state of charge (SOC) and pack current over time.

Table 3. gives a single-lap example: simulated energy (57.278 Wh) is within 1.505% of the measured value (58.154 Wh), with SOC, C-rate, and lap time consistent with expectations. Initial SOC was set to 85%.

Table 3. Measured and simulated values for a lap

Metric	Value	Unit
End-of-lap SOC	83.985	%
Specific energy	14.280	Wh/km
Estimated laps remaining	77.532	laps
Lap distance	4.011	km
Mean C-rate	0.210	C
Operating time needed	6.629	h
Lap time	307.811	s
Model lap energy	57.278	Wh
Measured lap energy	58.154	Wh
Test-model energy diff.	1.505	%

Table 4. shows measured and simulated energy consumption for 11 tours., the mean signed difference is −1.19%, the mean absolute percentage error is 2.81%, and the RMSE is 1.95 Wh. Larger deviations (e.g., Laps 4 and 8) plausibly reflect unmodeled effects such as localized shading, traffic interactions, or transient regeneration efficiency. Overall, the results indicate an agreement, sufficient for a solid basis for iESC strategy optimization.

Table 4. Multiple comparison of measured and simulated lap energies

Lap	Real Energy (Wh)	Model Energy (Wh)	Diff. (%)
1	61.665	60.430	2.004
2	63.050	63.832	-1.241
3	60.972	62.063	-1.790
4	64.239	60.956	5.111
5	58.013	59.757	-3.006
6	63.162	62.958	0.323
7	59.464	61.758	-3.858
8	54.844	58.275	-6.257
9	55.450	57.802	-4.241
10	58.154	57.278	1.505
11	66.069	67.123	1.505

4. Conclusion

This study presented a race-simulation and energy management framework for iESC that couples a physics-based vehicle model with real-time telemetry from the motor driver, BMS, and MPPTs. The formulation spans tractive forces, a surface-mounted PMSM with iq-based torque, an efficiency-map power path, and a pack-side balance with current/SOC update. Validation with ArıbaX showed close agreement: on a representative lap the model predicted 57.278 Wh vs. 58.154 Wh measured (error 1.505%), and across 11 laps the mean signed difference was −1.19%, mean absolute percentage error 2.81%, and RMSE 1.95 Wh sufficient fidelity for pacing and pit planning in the 24-hour format.

Future work will use this validated model for race strategy optimization and charge planning. These enhancements aim to keep strategy choices data-grounded and robust under real track conditions.

Acknowledgment

This study was supported by the Istanbul Technical University (ITU) Scientific Research Projects Unit (BAP) under LOKAP-A. Authors also acknowledge the use of OpenAI's ChatGPT to assist in improving the language clarity and organization of this study. The authors remain fully responsible for the content and technical accuracy.

5. References

[1] G. C. M. Arkesteijn, E. C. W. de Jong, and H. Polinder," Loss modeling and analysis of the Nuna solar car drive system," *Proc. Int. Conf. on Ecol. Veh. & Renew. Energies (EVER)*, Monaco, Mar./Apr. 2007,

[2] O. Ustun, M. Yilmaz, C. Gokce, U. Karakaya and R. N. Tuncay, "Energy Management Method for solar race car design and application," *2009 IEEE International Electric Machines and Drives Conference*, Miami, FL, USA, 2009, pp. 804-811

[3] E. Betancur, G. Osorio-Gomez, and J. C. Rivera," Heuristic´ optimization for the energy management and race strategy of a solar car," *Sustainability*, vol. 9, no. 9, Art. no. 1576, Sep. 2017

[4] E. Atmaca," Energy management of solar car in circuit race," *Turk. J. Elec. Eng. Comput. Sci*., vol. 23, no. 4, pp. 1142–1158, 2015

[5] I. A. Selin *et al*.," Building a time-optimal power consumption strategy for a solar car*," IOP Conf. Ser.: Mater. Sci. Eng*., vol. 643, no. 1, p. 012004, Sep. 2019

[6] H. C. Smith, S. Paterson, C. Mazzone, S. Diasinos, and G. Doig, "20 years of UNSW Australia's Sunswift solar car team: A new moment in the sun, but where to next?" *SAE Tech. Pape*r 2015-01-0073, 2015

[7] Ö. Üstün *et al*., "GÜNEŞ ENERJİLİ YARIŞ ARACININ ELEKTRİK TASARIM ÖLÇÜTLERİNİN, YOL PERFORMANS SİMÜLASYONUNUN ve ENERJİ YÖNETİM SİSTEMİNİN GELİŞTİRİLMESİ,"*ELECO 2006 - 4th National Symposium on Electrical Electronics and Computer Engineering}, Bursa, Turkey,* Dec. 2006.

[8] E. Yesil, A. O. Onol, A. Icke, and O. Atabay," Strategy optimization of a solar car for a long-distance race using Big Bang - Big Crunch optimization," *Proc. 14th IEEE Int. Symp. Comput. Intell. Inf. (CINTI)*, Budapest, Hungary, Nov. 2013

[9] S. Koçak, O. N. Atalay and A. F. Ergenc¸," An intelligent¨ driving strategy engine for a solar car," *Proc. 10th Int. Conf. Electrical and Electronics Engineering (ELECO)*, Bursa, Turkey, 2017, pp. 758–763.

[10] E. N. Mambou, T. G. Swart, A. R. Ndjiounge, and W. A. Clarke," Design and implementation of a real-time tracking and telemetry system for a solar car," *Proc. IEEE Int. Comput. Eng. Appl. Conf. (ICCEA)*, Mar. 2010, pp. 96–100,

[11] [11] A. Hilliard and G. A. Jamieson," Winning solar races with interface design," *Ergonomics in Design*, vol. 16, no. 2, pp. 6–13, Spring 2008, doi: 10.1518/106480407x312374.

[12] C. Oosthuizen et al.," Solar electric vehicle energy optimization for the Sasol Solar Challenge 2018," *IEEE Access*, vol. 7, pp. 175143–175158, Dec. 2019

[13] L. Bai et al.," Digital twin modeling of a solar car based on the hybrid model method with data-driven and mechanistic," *Appl. Sci*., vol. 11, no. 14, Art. no. 6399, Jul. 2021

[14] A. Akyildiz et al.," Optimum Selection of Lithium Iron Phosphate Battery Cells for Electric Vehicles," *IEEE Access*, vol. 13, pp. 55070–55080, 2025

[15] E. Uzun et al.," Comparison of Parameter Estimation Methods for Determining the Parameters of the Battery Electrical Equivalent Circuit Model," *Proc. 15th National Conf. Electrical and Electronics Engineering (ELECO)*, Bursa, Turkiye,2024